



Bukola Olalekan Bolaji

Mathematical Modelling and Experimental Investigation of Collector Efficiency of a Thermosyphonic Solar Water Heating System

The collector efficiency of a thermosyphonic solar water heating system was investigated theoretically and experimentally. Mathematical models were developed and used to predict the system performance. The solar collector with water pipes spreading across its width was also developed, tested and the theoretical results obtained agreed well with the experimental results. The collector efficiency is high especially around mid-day when the solar collector receives the highest energy. The results also reveal the dependency of the system performance on intensity of solar radiation and mass flow rate. Increase in both solar radiation and mass flow rate increases the collector efficiency. Maximum efficiencies of 72.8 and 70.4% were obtained from theoretical and experimental analyses, respectively, at optimum mass flow rate of 0.098 kg/s.

Keywords: *Solar, collector, efficiency, thermosyphonic, water heating*

1. Introduction

Solar energy is non-polluting, abundant and inexhaustible energy source. The solar thermal technology is a technology that is rapidly gaining acceptance as an energy saving measure in both domestic and commercial applications. It is fast becoming an alternative source of energy because of the high rate of depletion of the conventional energy sources. Solar energy is widely exploited for useful energy in the form of heat and electricity [1-3]. In the case of heating, solar water heaters have been investigated for many years. Most of them are classified by different operations; active and passive systems. The active system operates with forced circulation by using electric pump. The passive system operates with natural circulation and is often called the thermosyphon system [4-6].

All natural circulation systems are self-regulating; the greater the energy received, the more vigorous the circulation. The force that induces the circulation by overcoming the resistance of the system components is due to the difference in density of the hot water in the flow pipe and density of the cold water in the return pipe. The design of the flow pipe and heat transfer surface of the solar collector should be executed with the objective of achieving a high efficiency [7]. According to Bolaji [6], higher flow rate leads to higher collector efficiency. However, it also leads to high mixing in the storage tank and therefore, a reduction in the overall solar water heating system performance. The collector efficiency depends on many factors such as collector absorber material, absorber configuration, fluid medium and its properties, flow conditions (laminar or turbulent), and the overall heat loss value of the collector in which the absorber is built.

In this work, the efficiency for solar collector with water pipes spreading across its width is investigated theoretically and experimentally. A thermosyphonic water heating system was developed and tested, and the results obtained from the theoretical analysis are compared with those obtained from the experimental tests.

2. Mathematical Model Formulation for Collector Efficiency

The thermal performance of the collector of thermosyphon solar water heating system can be described by the energy balances on the collector absorber plate and the water in the collector flow tubes. The following assumptions are made in order to simplify the thermal analysis of the system in developing the steady state model [8]: (i) collector performance is under steady state conditions; (ii) flow tubes are parallel to each other and temperature gradients around tubes are negligible; (iii) the temperature drop between the top and bottom of the collector absorber plate and glazing is negligible; (iv) heat flow is one dimensional through the covers as well as through the back insulation; (v) thermo-physical properties of the materials are independent of temperature; and (vi) heat loss from the front and back of the absorber are to the same ambient temperature.

Consider the absorber plate with tube configuration as shown in Figure 1. The distance between the tubes is 'W', the tube diameter is 'D', and the absorber plate thickness is 'd'. Base on the above assumptions, the plate above the bond is at some local based temperature, T_b . The region between the centerline separating the tubes and the tube base can then be considered as a classical fin problem. The fin of length $(W-D)/2$ is shown in Figure 2, and an elemental region of width 'dx' for a unit length in the flow direction is shown in Figure 3. S represents $\alpha\tau I$, the absorbed solar energy per unit area (W/m^2). An energy balance on this element yield:

$$Sdx + U_L dx(T_a - T) + \left(-kd \frac{\partial T}{\partial x} \right) \Big|_x - \left(-kd \frac{\partial T}{\partial x} \right) \Big|_{x+dx} = 0 \quad (1)$$

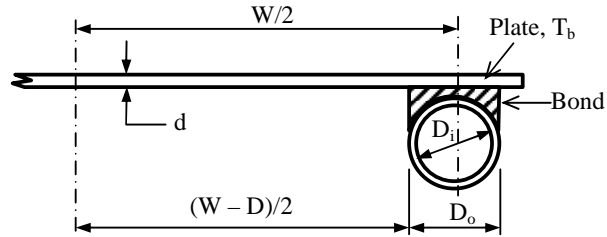


Figure 1. Absorber plate and tube dimensions

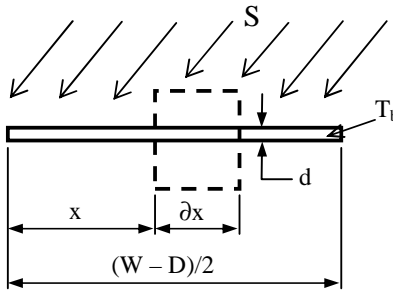


Figure 2. Fin element

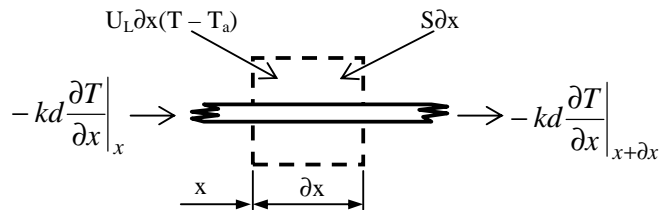


Figure 3. Energy balance on fin element

Dividing through by Δx and finding the limit as Δx approaches zero yields:

$$\frac{d^2 T}{dx^2} = \frac{U_L}{kd} \left(T - T_a - \frac{S}{U_L} \right) \quad (2)$$

The two boundary conditions necessary for this second order differential equation are symmetry at the centerline and known root temperatures:

$$\left. \frac{dT}{dx} \right|_{x=0} = 0 \text{ and } T|_{x=(W-D)/2} = T_b \quad (3)$$

If we define

$$m^2 = \frac{U_L}{kd} \quad (4)$$

and

$$\psi = T - T_a - \frac{S}{U_L} \quad (5)$$

Eq. (2) becomes

$$\frac{d^2\psi}{dx^2} - m^2\psi = 0 \quad (6)$$

which has the boundary conditions

$$\left. \frac{d\psi}{dx} \right|_{x=0} = 0 \text{ and } \psi|_{x=(W-D)/2} = T_b - T_a - \frac{S}{U_L} \quad (7)$$

The general solution is then

$$\psi = C_1 \sinh mx + C_2 \cosh mx \quad (8)$$

The constant C_1 and C_2 can be found by substituting the boundary conditions Eq. (7) into the general solution, Eq. (8). The results are:

$$\frac{T - T_a - \frac{S}{U_L}}{T_b - T_a - \frac{S}{U_L}} = \frac{\cosh mx}{\cosh m(W-D)/2} \quad (9)$$

The energy conducted to the region of the tube per unit of length in the flow direction can be found by evaluating Fourier's law at the fin base.

$$q_{fb} = -kd \left. \frac{dT}{dx} \right|_{x=(W-D)/2}$$

$$q_{fb} = \frac{kd m}{U_L} [S - U_L (T_b - T_a)] \tanh m(W-D)/2 \quad (10)$$

Eq. (10) account for the energy collected on only one side of a tube; therefore, for both sides and substitution of Eq. (4), the energy collection is

$$q_{fb} = (W-D) [S - U_L (T_b - T_a)] \frac{\tanh m(W-D)/2}{m(W-D)/2} \quad (11)$$

It is convenient to use the concept of a fin efficiency to rewrite Eq. (11) as

$$q_{fb} = (W-D) F [S - U_L (T_b - T_a)] \quad (12)$$

$$F = \frac{\tanh m(W - D)/2}{m(W - D)/2} \quad (13)$$

The function 'F' is the standard fin efficiency for straight fins with rectangular profile. The useful gain of the collector also includes the energy collected above the tube region. The energy gain for the tube region is

$$q_t = D[S - U_L(T_b - T_a)] \quad (14)$$

and the useful gain for the collector per unit of length in the flow direction becomes:

$$q_u = [(W - D)F + D][S - U_L(T_b - T_a)] \quad (15)$$

The useful gain from Eq. (15) must be transferred to the fluid. The resistance to heat flow to the fluid results from the bond and the fluid to tube resistance. The useful gain can be expressed in terms of these two resistances as:

$$q_u = \frac{T_b - T_f}{\frac{1}{h_{fi}\pi D_i} + \frac{1}{C_b}} \quad (16)$$

where D_i is the inside tube diameter and h_{fi} is the heat transfer coefficient between the fluid and the tube wall. The bond conductance, C_b , can be expressed as [9]:

$$C_b = \frac{k_b b}{\zeta} \quad (17)$$

T_b can be eliminated from consideration in order to obtain an expression for the useful gain in terms of known dimensions, physical parameters, and the local fluid temperature. Solving Eq. (16) for T_b , substituting it into Eq. (15), and solving the result for the useful gain per unit length, we obtain:

$$q'_u = WF' [S - U_L(T_{fi} - T_a)] \quad (18)$$

where F' is the collector efficiency factor and is given by

$$F' = \frac{1/U_L}{W \left\{ \frac{1}{U_L [D + (W - D)F]} + \frac{1}{C_b} + \frac{1}{\pi D_i h_{fi}} \right\}} \quad (19)$$

If collector has a length 'L' in the flow direction and the number of tubes in the collector is 'n' then the heat gained by the collector (Q_c) is found by multiplying Eq. (18) by Ln:

$$Q_c = WLnF' [S - U_L(T_{fi} - T_a)] \text{ or } Q_c = A_c F' [S - U_L(T_{fi} - T_a)] \quad (20)$$

where, $A_c = WLn$, the total collector area (m^2).

The useful energy gained by fluid flowing in the collector tubes (Q_u) is obtained by multiplying Eq. (20) by the collector flow factor (F'') [10]:

$$Q_u = A_c F' F'' [S - U_L (T_{fi} - T_a)] \quad (21)$$

The collector heat removal factor (F_R) is the product of collector efficiency factor (F') and collector flow factor (F''), therefore, Eq. (21) can be written as:

$$Q_u = A_c F_R [S - U_L (T_{fi} - T_a)] \quad (22)$$

The collector overall loss coefficient (U_L) is composed of the top and bottom losses. For single glass cover system, the top loss coefficient from the collector plate to ambient is obtained as [9]:

$$U_t = \frac{1}{R_{pg} + R_{gs}} \quad (23)$$

where, R_{pg} = the resistance to heat flow between plate and cover glass ($m^2.K/W$); and R_{gs} = the resistance to heat flow between cover glass and the surrounding ($m^2.K/W$). The complete formulation leading to the calculation of R_{pg} and R_{gs} is found in Duffie and Beckman [9]. The resistance to heat flow through the bottom of the collector is due to the insulation, and is obtained using Eq. (24):

$$U_b = k/z \quad (24)$$

Where k = insulation thermal conductivity ($W/m.K$); and z = insulation thickness (m).

$$\text{Therefore, } U_L = U_t + U_b \quad (25)$$

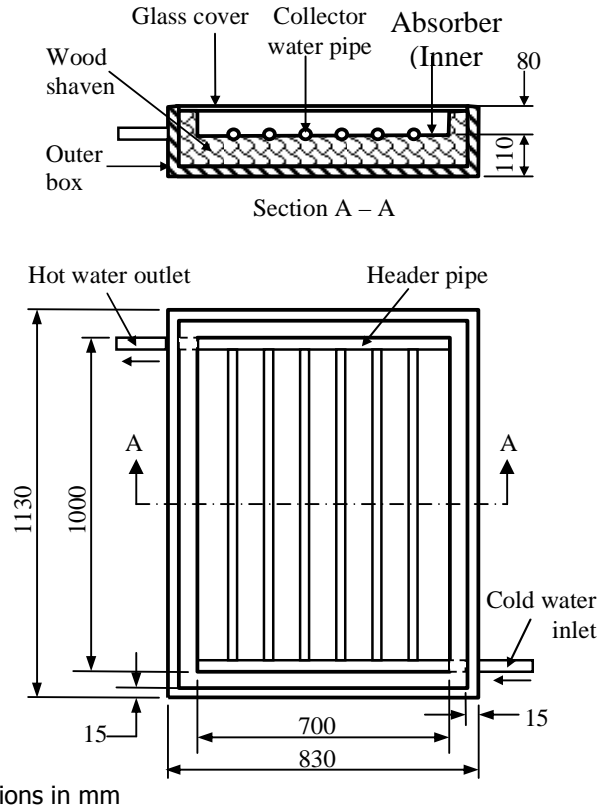
The overall heat loss coefficient (U_L) is used to estimate the heat gained by the collector (Q_c) and the useful energy gained by the fluid flowing in the collector tubes (Q_u) using Eqs. (20) and (22), while the collector efficiency (η_c) is obtained using Eq. (26):

$$\eta_c = \frac{Q_u}{A_c I} \quad (26)$$

The theoretical data were obtained by varying the different model inputs: temperature of the fluid inlet to collector (T_{fi}), ambient temperature (T_a) and solar radiation intensity (I).

3. Experimental Analysis

The solar water heating system consists of a flat-plate solar collector (Figure 4), storage tank and connecting pipes. The absorber steel plate of the solar collector was formed, like a corrugated sheet to accommodate the water pipes and headers in the grooves to maintain good contacts with the pipes. Each pipe is 1m long and has an inner diameter of 17 mm and outer diameter of 20 mm. The pipes are placed close together horizontally with a space of 83 mm in between and welded at both ends to the header pipes of 22 mm internal diameter, 25 mm outside diameter and 700 mm long each.



All dimensions in mm

Figure 4. Flat-plate solar collector with water pipes

The absorber-water pipe assembly formed an inner box, which in turns is mounted in an outer box, the space between the absorber-water pipe assembly and outer box is filled with glass wool as insulating material. The front surface of the box is then covered with 4 mm thick clear plain glass and air gap between the plate and the glass cover is 76 mm. The overall dimension of flat-plate solar collector is 1130 mm x 830 mm x 190 mm and the effective glazing area is 0.7 m². The connection between flat-plate collector and the storage tank are in two parts; the return pipe and the flow pipe. The return pipe connects the outlet of the storage tank and the inlet of the collector, while the flow pipe connects the outlet of the collector and the inlet of the storage tank together.

The flat-plate collector is orientated in such a way that it receives maximum solar radiation during the desired season of use. The best stationary orientation is due south in the Northern Hemisphere. In this position the inclination of the collector to the horizontal plane for the best all year round performance is approximately

10° more than the local geographical latitude. This approach was used in this work as a tilt angle of 17.25° was used for Akure, Nigeria location that is on latitude 7.25°N. The absorbing surfaces were painted with matt black paint. The absorbing plate and the absorbing surface of the pipes absorb solar radiation and the absorbed heat is then transmitted to the water in the pipes. Under the mode of natural convection the water flows through the pipes by the thermosyphonic force and enters the storage tank.

The thermosyphonic flow solar water heater was tested for 12 days at intervals of one hour between 8.00 h and 18.00 h each day. The incident solar radiation was measured with a Kipp and Zonen pyranometer, with accuracy of ±0.5%. The water inlet and outlet temperatures for the collector and storage tank as well as ambient air were measured with mercury-in-glass thermometers with a precision of 0.1°C.

4. Results and Discussion

Figure 5 shows the comparison of collector efficiency and incident solar radiation. The result shows that collector efficiency increases as the incident solar radiation increases for both theoretical and experimental analyses. This is a clear indication of the dependence of the system performance on the incident solar radiation. The efficiency obtained from theoretical analysis is slightly higher than that of experimental analysis. The average collector efficiency of 65.4% was obtained from theoretical analysis, while that obtained from experimental analysis was 64.1%.

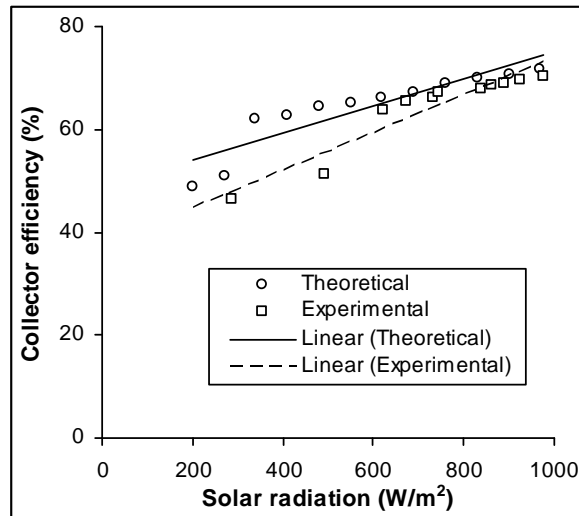


Figure 5. Variation of collector efficiency with incident solar radiation

Figure 6 shows the theoretical and experimental collector efficiencies versus collector performance coefficient $(T_{fi} - T_a)/I$. As shown in this figure, the collector efficiency increases as the collector performance coefficient decreases. The curves also show a good agreement between the theoretical and experimental results.

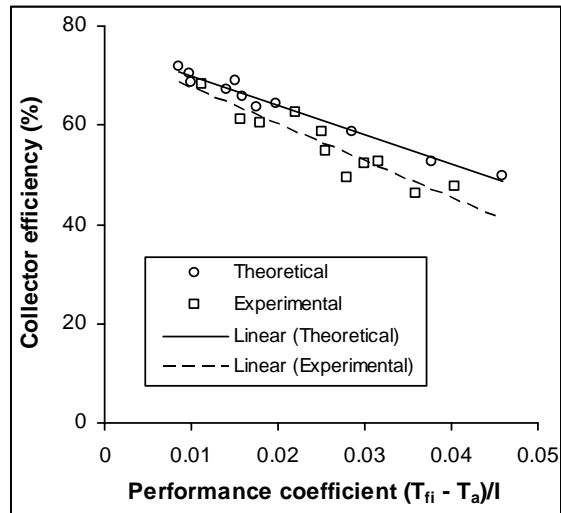


Figure 6. Variation of collector efficiency with performance coefficient $(T_{fi} - T_a)/I$

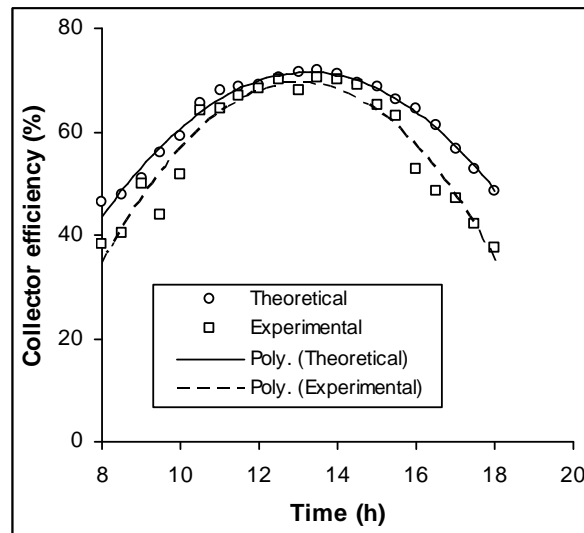


Figure 7. Hourly variation of collector efficiency

The theoretical and experimental results of variation of collector efficiency with time are shown Figure 7. As clearly shown in this figure, the collector efficiency is high especially around mid-day when the collector receives the highest energy, but it is low in the morning and late afternoon due to the low solar radiation during this period. Also, the slight difference observed between the theoretical and experimental results in the morning and late afternoon is due to the large angle of incidence of the sun during these periods, which impairs the operation of the collector. Beside this, the theoretical results agreed well with the experimental results.

Figure 8 shows the variation of the collector efficiency with the fluid mass flow rate. The results show the dependence of solar collector performance on the mass flow rate. This is in agreement with results obtained by Bolaji [6]. The collector efficiency increases as mass flow rate increases for both theoretical and experimental analyses until it reaches its maximum value after which any additional increase in the mass flow rate has no any effect on the performance of the solar collector. Maximum efficiencies of 72.8% (theoretical) and 70.4% (experimental) were obtained at optimum mass flow rate of 0.098 kg/s.

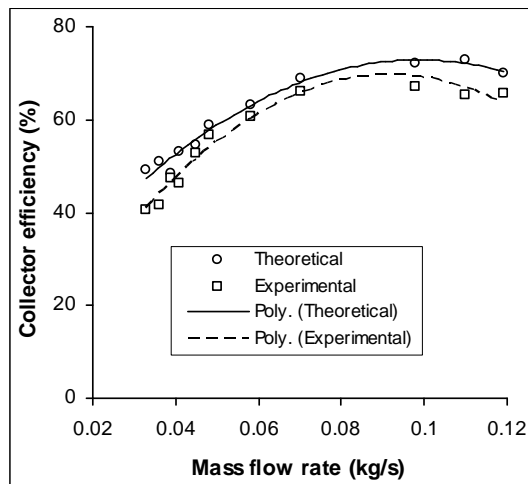


Figure 8. Variation of collector efficiency with mass flow rate

5. Conclusion

This paper investigates the collector efficiency of a thermosiphonic solar water heating system theoretically and experimentally. Mathematical models were developed and used for predicting the system performance. The solar collector with water pipes spreading across its width was also developed and tested and the results obtained were compared with those obtained in the theoretical analysis. The re-

sults obtained showed the dependency of the system performance on the incident solar radiation, the collector efficiency increases as the intensity of solar radiation increases.

The mathematical models predict results that compared reasonably well with the experimental data. The slight difference observed between the theoretical and experimental results in the morning and late afternoon is due to the large angle of incident of the sun during those periods, which impairs the operation of the solar collector. The collector efficiency is high especially around mid-day when the solar collector receives the highest energy. The results also reveal that the performance of the solar collector depends much on the mass flow rate. The collector efficiency increases as the flow rate increases until the maximum value is reached. Maximum efficiencies of 72.8 and 70.4% were obtained from theoretical and experimental analyses, respectively, at the optimum mass flow rate of 0.098 kg/s.

Nomenclature

A	area (m^2)	U_L	collector overall loss coefficient ($W/m^2.K$)
b	bond length (m)	W	distance between collector tubes (m)
C_b	bond conductance ($W/m.K$)	z	insulation thickness (m)
D	tube diameter (m)		
d	absorber plate thickness (m)		
F	standard fin efficiency	Greek:	
F'	collector efficiency factor	α	absorptivity
F''	collector flow factor	η	efficiency (%)
F_R	collector heat removal factor	ζ	bond average thickness (m)
h	heat transfer coefficient ($W/m^2.K$)	τ	transmissivity
I	solar radiation intensity (W/m^2)		
k	thermal conductivity ($W/m.K$)	Subscripts:	
L	collector length (m)	a	ambient
n	number of tubes	b	bond, bottom
Q	heat gain (W)	c	collector
q	heat gain per unit of length (W/m)	f	fluid
R_{gs}	resistance to heat flow between cover glass and the surrounding ($m^2.K/W$).	fb	fin-base
R_{pg}	resistance to heat flow between plate and cover glass ($m^2.K/W$);	i	inside
S	absorbed solar energy per unit area (W/m^2)	L	losses
T	temperature (K)	o	outside
		t	tube, top
		u	useful

References

- [1] Jansa, P., Chungpaibulpatana, S. & Limmeechokchai, B. (2004). A simulation model for predicting the performance of a built-in-storage solar water heater. *Thammasat International Journal of Science and Technology*, 9(4), 47-60.
- [2] Bolaji, B.O. & Adu, M.R. (2007). Design analysis of photovoltaic pumping system for rural application in Nigeria. *International Journal of Agricultural Sciences, Science, Environment and Technology, Series B*, 6(2), 120-130.
- [3] Bello, A.M.A., Makinde, V. & Sulu, A.T. (2010). Performance tests and thermal efficiency evaluation of a constructed solar box cooker at a Guinea Savannah Station (Ilorin, Nigeria). *Journal of American Science*, 6(2), 32-38.
- [4] Gaa, F.O., Behnia, M. & Morrison, G.L. (1996). Experimental study of flow rates through inclined open thermosyphons. *Solar Energy*, 57(5), 401-408.
- [5] Facao, J. & Oliveira, A.C. (2004). Analysis of a flat-plate heat pipe solar collector. *Proceedings of International Conference on Sustainable Energy Technologies*, June 1-5, Nottingham, UK, 28-30.
- [6] Bolaji, B.O. (2006). Flow Design and collector performance of a natural circulation solar water heater. *Journal of Engineering and Applied Sciences*, 1(1), 7-13.
- [7] Sekhar, Y.R., Sharma K.V. & Rao, M.B. (2009). Evaluation of heat loss coefficients in solar flat plate collectors. *ARPN Journal of Engineering and Applied Sciences*, 4(5), 15-19.
- [8] Bolaji, B.O. (1998). *Performance Evaluation of an Improved Thermosyphon Solar Water Heating System*. M.Eng. Thesis in the Department of Mechanical Engineering, Federal University of Technology, Akure, Nigeria.
- [9] Duffie, J.A. & Beckman, W.A. (1991). *Solar engineering of thermal processes*. 2nd Edition, John Wiley and Sons New York.
- [10] Ismail, K.A.R. & Abogderah, M.M. (1998). Performance of a heat pipe solar collector. *Journal of Solar Energy Engineering, Transactions of the ASME*, 120, 51-59.

Address:

- Dr. Eng. Bukola Olalekan Bolaji, "Department of Mechanical Engineering" University of Agriculture, P.M.B. 2240, Abeokuta, Nigeria, bobbolaji2007@yahoo.com